A CONDUCTIVITY PROBE FOR MEASURING LOCAL CONCENTRATIONS IN SLURRY SYSTEMS

H. Nasr-El-Din,† C. A. Shook and J. Colwell

Department of Chemical Engineering, University of Saskatchewan, Saskatoon,
Saskatchewan S7N OWO, Canada

Abstract—A simple, economical and accurate technique has been developed to measure local *in situ* solids concentration in slurry systems. The instrument relies on measuring slurry resistivity, as it changes with the solids concentration, for a small region in space. The device was tested in comparison with isokinetic sampling and γ-ray absorption for a variety of slurry pipeline flows. The effects of fluid properties, temperature, velocity, particle size and pipe wall material were examined experimentally. In contrast with previous techniques the effect of fluid velocity upon the measurements was eliminated by a dual electrode-pair system.

INTRODUCTION

Slurry pipelines and other slurry-handling devices are widely used in the chemical and mineral industries. The solids concentration is often of great importance to the operator of such equipment. If the concentration is known one can begin to understand the internal flow structure which governs the performance of the system. Some of the phenomena which depend upon solids concentration include: corrosion/erosion, pressure drops and power requirements in slurry pipelines.

A number of methods have been used to measure solids concentrations. Reviews of these methods are given by Kakka & Phil (1974), Debreczeni *et al.* (1978), Kao & Kazanskij (1979) and Baker & Hemp (1981). Generally speaking, these methods seek to find a specific property which is significantly different for the two phases. The value of this property for the mixture will then depend on the solids concentration. By measuring this property one should be able to find the solids concentration from a calibration curve. Examples of the specific property are density, electrical conductivity, dielectric constant and absorption of electromagnetic radiation. Any of these methods will give inaccurate measurements if the specific properties of the two phases approach one another or if the solids concentration is very low. Depending on the system geometry and the method, the various methods give the solids concentration over different volumes in space. In terms of the volume over which the solids concentration is averaged, methods of measuring solids concentration can be divided into three categories.

The first category includes methods which give concentrations averaged over a large volume of space such as a length of pipe. Examples in this category are the vertical counterflow meter, inclined and straight pipe concentration meters (Debreczeni *et al.* 1978).

The second category gives a concentration averaged along a line such as a chord spanning the pipe. Examples of these methods are: collimated γ-ray beam absorption (e.g. Kakka & Phil 1974), ultrasonic methods (Ong & Beck 1975), autocorrelation of scattered laser light (Stanley-Wood *et al.* 1981) and a conductivity method (Lee *et al.* 1974).

The third category gives the solids concentration over a small volume in space. The group includes isokinetic sampling and the photographic method of Scarlett & Grimley (1974). For isokinetic sampling, the volume depends on the probe inside diameter.

Since the present study deals with a conductivity probe, a brief review of previous work on electrical methods is of interest. The specific property in these methods is either the conductivity or dielectric constant. These methods have the advantage that they give a continuous reading. This means that they could be used as a measuring element in a control loop.

Electrical methods have been used successfully not only in solid–liquid systems but also in gas–liquid and three-phase systems. In gas–liquid systems, both conductivity methods and

---

†Present address: Chemical Engineering Department, University of Alberta, Edmonton, Alberta T6G 2G6, Canada.

capacitance methods have been used to measure the air or steam void fraction (Cybula 1971; Merilo et al. 1977; Subbotin et al. 1974; Beck et al. 1983). In a three-phase fluidized bed, Begovich & Watson (1978) used a conductivity method to measure axial distributions of air and water.

For slurry systems, both conductivity and capacitance methods have been used. Capacitance methods were used by Keska (1978) and Green & Cunliffe (1983). Conductivity methods were used for slurry systems of conducting liquids (Beck et al. 1971; Ong & Beck 1975). These studies have shown that measuring the solids concentration from conductivity noise is possible. This work was done with two opposing electrodes mounted on the pipe wall. After processing, the signal from these electrodes was used to measure concentrations. In order to eliminate the effect of polarization resistance on the electrode surfaces, a large ballast resistance was used. Also, a filter of bandwidth 1–1000 Hz was included to eliminate the effect of liquid chemical composition and temperature on the measurements. Lee et al. (1974) used the same method to measure small quantities of a non-conducting liquid in a conducting one. These measurements were made in a stirred tank. It was found that the calibration curve depended on the stirrer speed. As the stirrer speed increased, the corresponding field voltage increased. This was related to the increase of turbulence with the stirrer speed. A simple theoretical analysis was given to show the relation between the change of mixture resistance and the solids concentration. Although the analysis indicated a linear relationship, the experimental results showed non-linearity.

Beck et al. (1974) measured the solids concentration in a 2.5 cm pipeline using two tandem electrodes at the bottom of the pipe. For a sand–water slurry, they also found the calibration curve to be non-linear and dependent on velocity. Kazanskij (1977), as reported by Kao & Kazanskij (1979), measured solids concentration using three or more pairs of electrodes mounted on the pipe wall.

In previous work, although electrodes of various shapes and locations were used, a common factor is that the electrodes were fixed on the pipe wall: either diametrically opposed or axially displaced (tandem). The advantage of these arrangements is that no electrodes intrude or obstruct the flow. On the other hand, they have the following disadvantages: (i) One can not study the solids distribution over the pipe cross section. This distribution is extremely important for slurry pipelines, where one often finds a substantial variation in the solids concentration from the top to the bottom of the pipe. (ii) One can not eliminate the effect of velocity on the calibration curve. This effect is very complicated because by changing the velocity, the solids distribution across the pipe changes. Simultaneously, the velocity distribution and turbulence pattern will change and this will alter the polarization resistance on the surfaces of the electrodes. The effect of these changes on the calibration curve is difficult to predict.

The object of the present study was to develop a conductivity probe to measure the solids concentration for a small volume in space; to find an efficient procedure to calibrate it; and, finally, to test the probe against other accepted techniques for measuring solids concentration.

SLURRY ELECTRICAL CONDUCTIVITY

Since the principle of the probe is to determine the solids concentration from the variation of slurry conductivity, it is useful to list some known expressions for the effect of concentration on slurry conductivity. In general terms, the electrical conductivity of a liquid–solid system depends on the electrical conductivities of the two phases and their relative amounts. Maxwell (1881) was the first to investigate the phenomenon, and derived the following expression:

$$\frac{K_m - K_l}{K_m + 2K_l} = C \frac{K_s - K_l}{K_s + 2K_l}, \qquad [1]$$

where C is the solids concentration, K_m, K_s and K_l are the conductivities of the mixture, dispersed and continuous phases, respectively. This equation is valid for spherical particles of uniform size at low concentrations. One observes that the mixture conductivity does not follow the additivity rule, i.e. the relation between the mixture conductivity and the concentration of the dispersed phase is not linear.

Based on the analogy between heat and current flows, Tareef, as reported by Perry & Chilton

(1973), and also Hashin (1968), as reported by Neale & Nader (1973), derived the following expression:

$$K_m = K_l \left[\frac{2 K_l + K_s - 2(K_l - K_s)C}{2 K_l + K_s + (K_l - K_s)C} \right].$$ [2]

One notices that [2] is equivalent to Maxwell's equation. For a mixture of a non-conducting solids ($K_s = 0$) in a conducting liquid phase (the case of interest in this study), Maxwell's equation gives:

$$K_m = K_l \frac{2(1 - C)}{(2 + C)}.$$ [3]

One observes from [3] that the mixture conductivity equals that of the liquid at $C = 0$. At $C = 1$, the mixture conductivity is zero. Turner (1973, 1976) measured the conductivity of liquid fluidized beds of conducting and non-conducting solids. For the latter, he found that the relation between the mixture conductivity and solids concentration followed Maxwell's equation for spherical particles even at high concentrations where Maxwell's assumptions were not valid. Neale & Nader (1973) also found that Maxwell's equation gave excellent predictions for suspensions of non-conducting spheres at solids concentrations up to 55%.

Bruggeman (1935) extended Maxwell's work to the case of spheres of various sizes and random distribution. His equation should, therefore, be valid for a mixture of a wide size distribution at any concentration. For a mixture of solids conductivity K_s, liquid conductivity K_l and solids concentration C, Bruggeman's equation is

$$(K_m - K_s)\left(\frac{K_m}{K_l}\right)^{-1/3} = (1 - C)(K_l - K_s).$$ [4]

For a mixture of nonconducting solids in a conducting liquid, this reduces to

$$K_m = \bar{K_l} \cdot (1 - C)^{3/2}.$$ [5]

De la Rue & Tobias (1959) measured the conductivities of random suspensions of spheres, cylinders and sand particles in aqueous solutions of zinc bromide of approximately the same densities as the particles. They found the suspension conductivity could be calculated from the following expression:

$$K_m = K_l \cdot (1 - C)^m,$$ [6]

where $m = 1.5$ for a solids concentration in the range of 0.45–0.75. One should mention that this equation is similar to that of Bruggeman (1935).

Begovich & Watson (1978) found experimentally that the mixture conductivity in a liquid–solid fluidized bed is proportional to the liquid holdup. Their equation can be written as

$$K_m = K_l \cdot (1 - C).$$ [7]

Still another expression was given by Machon et al. (1982):

$$K_m = K_l \cdot (1 - kC),$$ [8]

where k is a constant to be determined experimentally. Machon et al. found this constant by measuring the conductivity of a bed of non-moving particles. The bed solids concentration was in the range of 0.6–0.65. Equation [8] is linear and according to this equation, K_m equals K_l for $C = 0$; this is similar to [3]. However, at $C = 1$, [8] does not agree with Maxwell's prediction unless $k = 1$. This observation and the fact that it has no theoretical justification suggests that [8] should be used with caution.

A comparison of these expressions is given in table 1. This table shows the increase in slurry resistance because of the presence of non-conducting solids, $(R_m - R_l)$ divided by fluid resistance as a function of solids concentration. R_m and R_l are the slurry and fluid resistances, respectively. One observes that Maxwell's and Bruggeman's relations give very similar results at low solids concentrations. At higher concentrations, Bruggeman's relation gives higher values. One also notices that Begovich & Watson's (1978) relation predicts lower values for all concentrations and the deviation from the other two relations increases as the concentration increases.

Table 1. Comparison between various expressions for slurry resistance

	$(R_m - R_i) R_i$		
C (%)	Begovich & Watson (1978)	Maxwell (1881)	Bruggeman (1935)
10	0.111	0.167	0.171
20	0.25	0.375	0.398
30	0.429	0.643	0.708
40	0.667	1.0	1.152
50	1.0	1.5	1.829
60	1.5	2.05	2.953
70	2.33	3.5	5.086
80	4.0	6.0	10.18
90	9.0	13.5	30.623
100	Infinite	Infinite	Infinite

PROBE DESCRIPTION

The probe, shown in figure 1, has an L-shaped configuration. It was constructed from 3/16″ stainless-steel tubing. To minimize the effect of flow disturbances, the probe terminates with a conical stainless steel tip and the approach length to the sensor electrodes is 10 probe diameters. The two field electrodes are flush with the surface of the tubing and completely insulated from each other. The field electrode of larger area is grounded to the pipeline. The field electrode circuit consisted of a function generator, a ballast resistance and an ammeter. The two sensor electrodes are also flush with the surface of the tubing, 1 mm apart, and are located between the field electrodes. The sensor electrodes were constructed from 28 G platinum. They are also completely insulated from each other and from the field electrodes. The sensor electrodes are connected to a voltmeter from which a time-averaged reading can be obtained.

The probe as described above has two unique features:

(a) The field electrodes are mounted on the probe itself and not on the pipe wall, as commonly used (e.g. Lee et al. 1974). This feature is very important because it eliminates the need for higher voltages for measurements in large pipes. It also allows one to study the solids distribution within the pipe.

(b) The potential is sensed for a small region (1 mm dia) in the applied field. This means that resistivity and solids concentration can be measured over a small volume in space.

PROBE OPERATION

The operation of the probe relies on the variation of the slurry resistivity as the solids concentration changes. To understand the probe's principle, we first assume the probe is
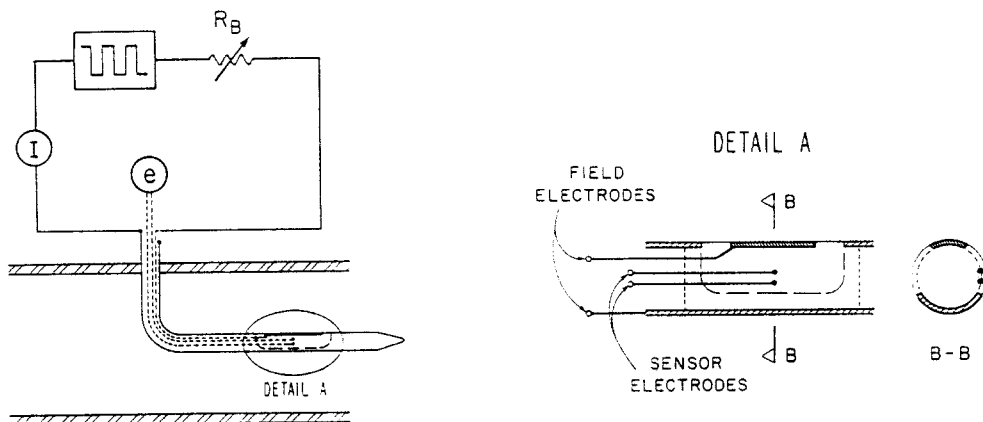

Figure 1. Conductivity probe.

surrounded by a conducting liquid such as tapwater, then if one applies a potential across the field electrodes (of the order of 5 V) a small current will flow from one field electrode to another. The value of this current, for a fixed geometry and applied signal, depends on the total resistance of the medium surrounding the field electrodes. If one adds non-conducting particles (e.g. sand particles) to this fluid, then the resistivity of the mixture will increase. As the solids concentration increases, the resistivity increases and consequently the field circuit current will decrease. One way of measuring the solids concentration, similar to that used by previous workers, would be to relate this current change to the solids concentration. One should note that this method has a serious disadvantage because the current depends on both the slurry resistivity and the polarization resistance developed on the surfaces of the field electrodes. This polarization resistance is velocity dependent. Using this method one obtains calibration curves which are functions of velocity (e.g. Lee et al. 1974).

To avoid this problem, it was decided not to use the total current to measure the solids concentration. Instead we measure the voltage across the two sensor electrodes located between the field electrodes, as shown in figure 1. Since the impedance of the sensor circuit is virtually infinite, practically no current flows into the sensors. Consequently, no polarization occurs on their surfaces. Thus, one should find a calibration curve which is independent of velocity.

To minimize the effect of polarization of the field electrodes and facilitate constant-current operation, a ballast resistance was used in the field electrode circuit. Also, to eliminate fluid electrolysis, a square wave of 1 kHz and 5 V amplitude was used. This gave 1 mA with ballast resistances of the order of 4000 Ω. These values were used for all the measurements of the present study.

EXPERIMENTAL SETUP

As shown in figure 2, the loop consists of a 5 cm (nominal) i.d. aluminium pipeline, a pump driven by a variable-speed motor, a heat exchanger to remove energy dissipated during flow and to control loop temperature, a magnetic flowmeter, a stand tank and a rotatable test section. The rotatable section was constructed from transparent acrylic pipe which allowed visual observation. The rotatable section allowed measurements to be made at various positions within the pipe.

In some tests, the conductivity probe was replaced by a sampling probe to measure in situ local concentrations The sampling probe also had an L-shaped configuration. It was constructed from 3/8″ stainless-steel tubing with an i.d. of 8 mm and a probe nozzle length of 7 probe radii. In order to eliminate the errors associated with blunt and straight probes (Nasr-El-Din & Shook, 1985), the probe had a relative wall thickness of 0.025 and a taper angle of 5°. Previous studies (Nasr-El-Din et al. 1984) have confirmed the reliability of this sampling technique.
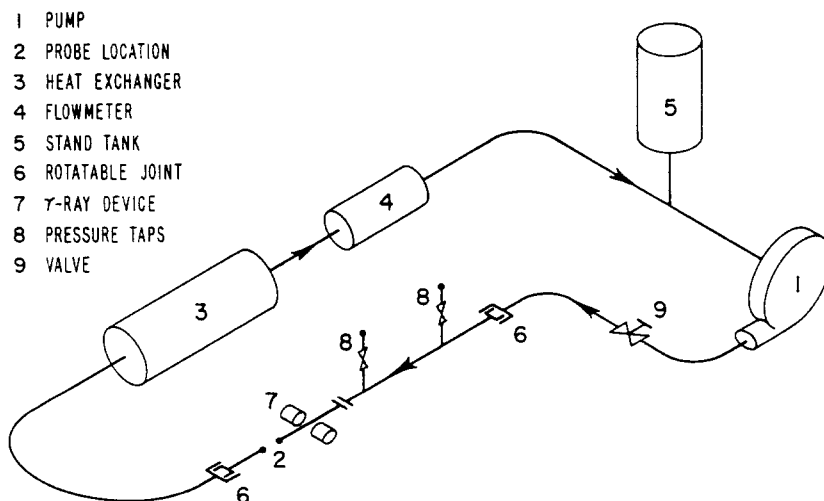
1 PUMP
2 PROBE LOCATION
3 HEAT EXCHANGER
4 FLOWMETER
5 STAND TANK
6 ROTATABLE JOINT
7 γ-RAY DEVICE
8 PRESSURE TAPS
9 VALVE

Figure 2. Experimental setup.

Particles	Mean diameter (mm)	Density (g/cm³)	Shape
Glass beads	1.5	3.0	Spherical
Glass beads	2.8	2.5	Spherical
Glass beads	5.5	2.3	Spherical
Polystyrene	0.3	1.05	Spherical
Polystyrene	1.4	1.06	Irregular
Fine sand	0.19	2.65	Irregular
Medium sand	0.45	2.65	Irregular
Coarse sand	0.9	2.65	Irregular

Solids concentrations at various distances from the pipe bottom were also measured using a γ-ray absorption method with a ^{137}Cs source and a scintillation counter detector. This γ-ray method gives chord-average concentrations, whereas the conductivity probe and the sampling probe will give local *in situ* values.

The particles used in this study were sands, glass beads and polystyrene particles. Table 2 summarizes their properties. The continuous phase was mainly tapwater. The resistivity of tapwater was 2720 Ω cm at 25°C.

The volume of the loop was measured by adding weighed amounts of water to fill it. The required solids concentrations were obtained by adding the corresponding amounts of solids. Bulk velocities were measured by the magnetic flowmeter connected to an LSI-11 minicomputer for data recording.

The experimental work in this study covered the effects of operating conditions on the conductivity probe, various methods for calibrating the probe and, finally, testing the conductivity probe measurements against measurements obtained by isokinetic sampling and γ-ray absorption.

EXPERIMENTAL RESULTS

The first operating parameter tested was that of probe position. The conductivity probe was mounted on the rotatable section (acrylic), the loop was filled with tapwater and the voltage drop across the sensor electrodes was measured by moving the probe in the vertical plane from the bottom of the pipe $[Y = (y/D) = 0]$ to the top $(Y = 1)$, where y is the distance measured from the bottom of the pipe and D is the pipe inside diameter. One should notice that if the probe is traversed downward, as it approaches the bottom of the pipe, the field electrode with the larger area is closer to the pipe wall. On the other hand, when the probe approaches the top of the pipe, the small-area electrode is closer to the wall. Sensor potential measurements were done at a constant field circuit current of 1 mA.

Figure 3 shows the measured voltage as a function of position $e(0, Y)$ normalized by the voltage value at the pipe center $e(0, 0.5)$. We observe that the voltage profile is asymmetrical. Although it
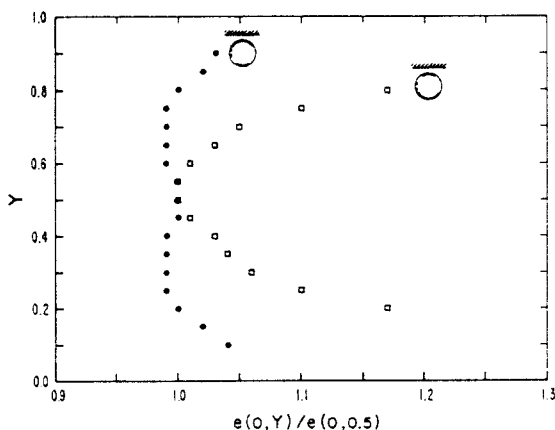

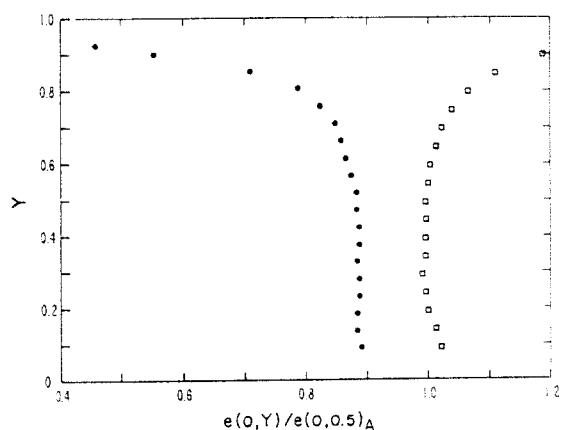Figure 3. Effect of probe position and the wall–electrode configuration.

Figure 4. Effect of pipe wall material on potential: □, acrylic pipe; ●, steel pipe.

is almost independent of position from $Y = 0.2$ to 0.6, outside this range the voltage increases as the probe approaches the pipe wall. This increase in voltage is a function of the area of the field electrode closer to the wall. Approaching the pipe wall with the large-area electrode shows an increase of 4% at $Y = 0.1$. On the other hand, approaching the wall with the small-area electrode shows a 17% increase at $Y = 0.8$. Measurements closer to the wall were not possible because of the physical size of the probe.

These results can be explained as follows. Generally speaking, the presence of an insulating wall obstructs the flow of current by confining the conducting region. With a given total field current, the current in the vicinity of the sensor electrodes is increased. Consequently, the sensor voltage will be higher. Obviously, this effect is a function of the electrode area nearest the wall. The larger area will compensate for some of the increase in the field circuit resistance because of the presence of an insulating wall.

Two main conclusions could be drawn from these results; first, to get a symmetrical profile in a uniform medium, one must always approach the pipe wall with the same electrode. Secondly, the conductivity of the pipe wall should have a significant effect on the measurements, especially when the small-area electrode approaches the pipe wall. Approaching the pipe wall with the same electrode could be done in these experiments by rotating the pipe 180° about its axis. For all subsequent measurements, the large-area electrode was the one closest to the pipe wall. In addition to showing less variation of sensor voltage with position, because of probe geometry, one could get much closer to the pipe wall.

The variation of sensor voltage, shown in figure 3, suggested that the effect of the pipe wall conductivity should be examined. To achieve this, the probe was mounted in a 5 cm (nominal) steel pipe and measurements were made in tapwater. Figure 4 shows the voltage measurements for the steel pipe (conducting wall) and the acrylic pipe (insulating wall). Both are normalized with the voltage value at the pipe center of the acrylic pipe $e(0,0.5)_A$. One observes that the voltage measurement for the steel pipe at any position is lower than the corresponding value for the acrylic one. This decrease occurs because the current can flow to the whole wall. Of course it also minimizes any resistance increase caused by confining the current flow. In this case, approaching the pipe wall with the large-area electrode has no significant effect on the sensor voltage. With the large-area field electrode grounded, as in the present study, approaching the pipe with the small-area electrode shows a drastic drop due to the short-circuiting of the sensor electrode region.

The results in figure 4 indicate that the probe can be used in conducting pipelines without correcting for the effect of position relative to the pipe wall. For non-conducting pipes, such as the one used in the rest of this study, one must correct for this small positional effect.

The effect of velocity was studied thoroughly by taking measurements in the acrylic pipe in the velocity range of 0–4 m/s. Tapwater was used in these experiments at closely controlled loop temperatures. Table 3 shows the means and standard deviations for the sensor voltage mea-

Table 3. Normalized sensor voltages as a function of position measured over a velocity range of 0–4 m/s

Position (Y)	$\dfrac{e(0,Y)}{e(0,0.5)}$	Standard deviation
0.1	1.03	0.009
0.15	1.02	0.005
0.2	1.0	0.005
0.25	0.99	0.007
0.3	0.99	0.005
0.35	0.99	0.006
0.4	0.99	0.005
0.45	1.0	0.005
0.5	1.0	—
0.55	1.0	0.007
0.6	0.99	0.007
0.65	0.99	0.007
0.7	0.99	0.007
0.75	0.99	0.008
0.8	1.0	0.007
0.85	1.02	0.007
0.9	1.04	0.01

surements, normalized by the value at the center of the pipe. These results were obtained from 15 experiments. One observes, in contrast with previous work, that the effect of velocity is insignificant. This result is of great importance because it shows that the method of measuring voltages between sensor electrodes, instead of field electrodes, eliminates velocity effects. This implies that one can obtain a probe calibration curve which is independent of velocity. This is important in measuring the solids distribution in pipelines because it eliminates the need to determine local velocities in order to measure solids concentrations.

The effect of temperature was tested in the range of 8–25°C. Measurements were made for tapwater ($C = 0$) at the pipe center. Figure 5 shows these results. As temperature increases, the water resistivity decreases and so does the sensor voltage. Examining these results using a least-squares method has shown that the voltage decreases with rising temperature at 2%/deg. This value agrees with previous experimental work (Cybula 1971; Turner 1973). It is evident that the temperature has a significant effect on the measurements and its effect should be considered when the probe is used to measure solids concentration.

PROBE CALIBRATION

Various methods were used to calibrate the probe. These studies were conducted to find the relation between voltage (e) and solids concentration (C), for comparison with those of Maxwell and Bruggeman. It was also necessary to establish an efficient probe calibration procedure.

The first test was conducted with the conductivity probe mounted in the pipeline shown in figure 2. Polystyrene particles of 0.3 mm mean dia were used in these slurries. These particles were chosen because of their tendency to give a uniform concentration profile across the pipe. Concentrations were obtained by isokinetic sampling at the center of the pipe over a temperature range of 8–25°C. Figure 5 shows the results, the effect of temperature in tapwater is shown for comparison. One observes that at a fixed temperature, increasing solids concentrations cause the sensor voltage to increase. This result is reasonable because polystyrene particles are non-conducting and their presence increases slurry resistivity.

One also observes that the curves obtained at various concentrations are almost parallel. This means that the rate of change of voltage with respect to temperature is independent of the solids concentration. By cross-plotting the results shown in figure 5, one can prepare a set of calibration curves with temperature as a parameter. When this was done, it was found that the value of e at $C = 0$, obtained by extrapolation, was lower than the corresponding value obtained for tapwater at the same temperature. After reviewing the procedure of this experiment, it was concluded that the only possible reason for this difference was the fact that a small amount of wetting agent was added with the solids to increase the wettability of the polystyrene particles. To check this effect, the loop was operated using tapwater, measurements were taken at various surfactant concentrations (C_d). Figure 6 shows the results obtained. One observes that, at a given
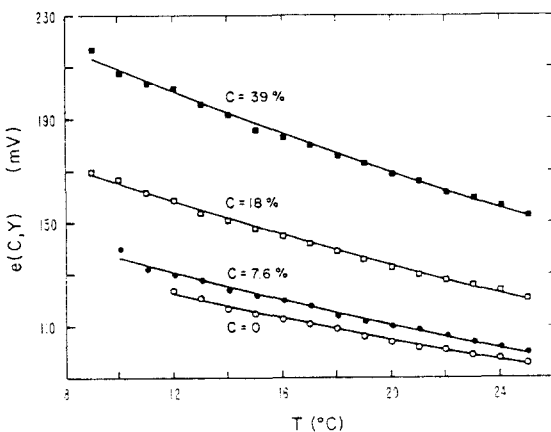

Figure 5. Effect of temperature on measured potential: polystyrene particles. $d = 0.3$ mm, $Y = 0.5$.
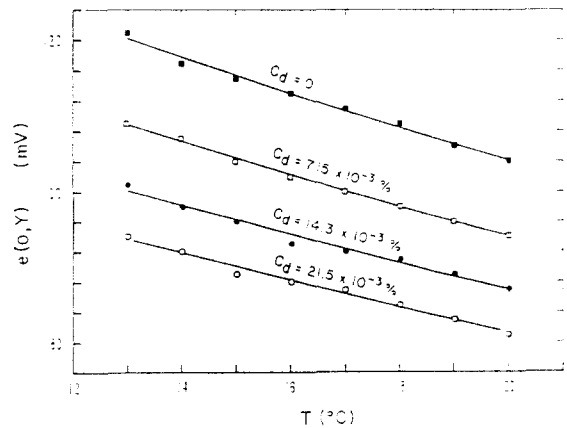
Figure 6. Effect of surfactant in the water on potential. $Y = 0.5$.

temperature, as the surfactant concentration increases the voltage decreases. This decrease is reasonable since the surfactant contains sodium salts of organic acids. Its presence would decrease the fluid resistivity and consequently the sensor voltage. These results show: (i) a calibration curve based on these measurements is not acceptable because of poor control on the amount of surfactant; and (ii) the voltage measured is strongly affected by any small change in the chemical composition of the conducting liquid.

The results shown in figures 5 and 6 indicate that using e as a measure for solids concentration is not appropriate, because it is strongly dependent on temperature, chemical composition and position. It was decided therefore to use the following function in calibrating the probe: $[e(C,Y) - e(0,Y)]/e(0,Y)$. This will correct the sensor voltage at any concentration (C) for temperature, chemical composition and position in the pipe.

Sedimentation was the second method tested to calibrate the probe. Polystyrene particles of 0.3 mm mean dia were again used, without the wetting agent. These particles were chosen because of their very low settling velocities, which allowed sufficient time for voltage readings. Tests were done in a 5 cm acrylic pipe using both tapwater and a glycol solution of the same density as the particles.

Figure 7 shows the voltage measurements, expressed in terms of the function defined above vs concentration in the two fluids. Maxwell's relation is also shown for comparison. The figure indicates good agreement between the experimental measurements and Maxwell's relation. We observe that although Maxwell's relation was supposed to be valid for low concentrations, it actually agrees very well with all the experimental results. This observation agrees with previous work (Turner 1973; Neale & Nader 1973; Merilo $et\ al.$ 1977). One also observes that changing the solution conductivity has no effect on the measurements. This demonstrates that by using the concentration function, one should be able to isolate the effects of all variables except C.

The second step was to examine the effect of particle size on the calibration curve. This was not possible by sedimentation, since coarser particles have higher settling velocities. It was therefore decided to use a liquid–solid fluidized bed. A 5 cm acrylic pipe was used to construct a fluidization column. Weighed quantities of solids were used and solids concentrations were varied by changing the liquid flowrate. Measurements for these experiments included voltage, bed height and temperature. To allow a precise determination of concentration from bed height, narrow sizes of particles were used.

Figure 8 shows the experimental data obtained for a sand fraction of 0.6 mm mean dia and narrow size distribution. This sand fraction was obtained from the medium sand (table 2) by screening several times. Measurements in this experiment were taken at the pipe center. Maxwell's and Bruggeman's relations are shown for comparison. One observes good agreement at low concentrations with both relations. At high solids concentrations, the experimetnal data exceed Maxwell's predictions but show good agreement with Bruggeman's equation.
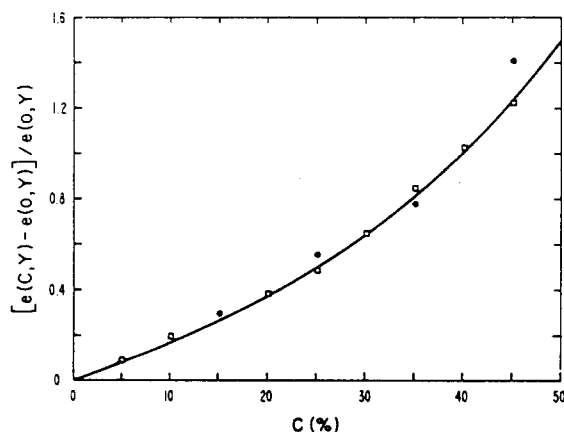

Figure 7. Probe calibration in sedimentation tests. —, Maxwell's relation; □, polystyrene/water; ●, polystyrene/glycol solution; $d = 0.3$ mm, $Y = 0.5$.
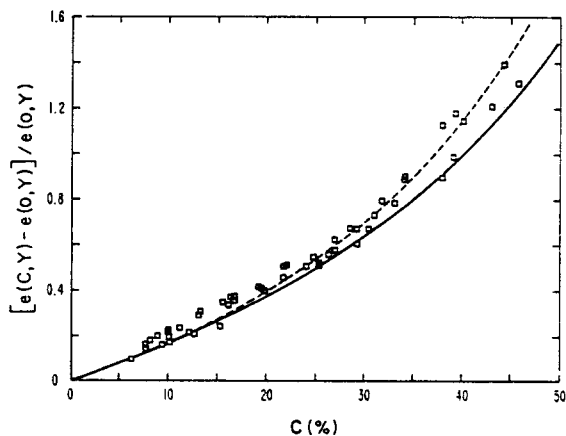
Figure 8. Probe calibration in fluidization tests. - - -, Bruggeman's relation; —, Maxwell's relation; □, sand particles $d = 0.6$ mm; $Y = 0.5$.
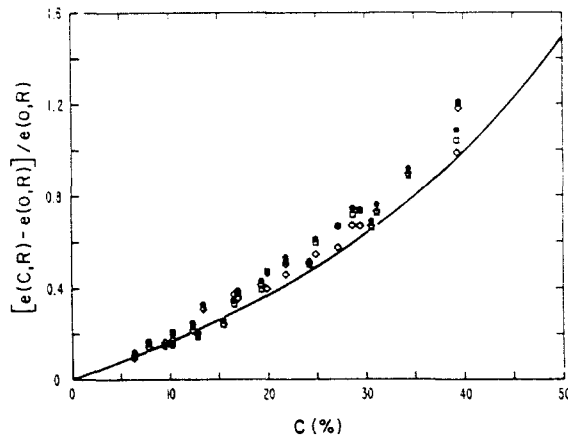
Figure 9. Effect of probe position on the calibration curve using sand, particles $d = 0.6$ mm. —, Maxwell's relation; $\Diamond$, $R = 0.0$; $\square$, $R = 0.7$; $\bullet$, $R = 0.8$.

From figures 7 and 8, one can conclude that particle shape has an effect on the results. One notices good agreement between the experimental results for spherical particles (0.3 mm polystyrene particles) and Maxwell's equation. For irregular sand particles Maxwell's equation underpredicts the experimental results, especially at high concentrations. One also notices that the scatter in the experimental data is higher for sand particles than for polystyrene particles. The scatter increases for sand particles as concentration increases. It seems from this observation that it is difficult to reproduce the same particle packing for irregular particles.

Figure 9 shows measurements for the same sand fraction at radial positions of $R = 2r/D = 0.0$, 0.7 and 0.8, where r is the radial position measured from the pipe center. One observes that the effect of position on $[e(C,R) - e(0,R)]/e(0,R)$ is insignificant. Results obtained at the other positions show the same deviation from Maxwell's relation at higher concentrations.

Because measurements refer to a small volume in space, the effect of particle size was of interest. This was examined through two sets of experiments. In the first test, sand fractions of 0.6 and 1.5 mm mean dia were used. These sand fractions were obtained from the medium and coarse sands (see table 2), respectively. In the second, glass beads of 1.5, 2.8 and 5.5 mm mean dia and spherical shape were used.

Figure 10 shows the results obtained for the sand particles. One observes that the coarser particles show the same deviation at high concentration from Maxwell's equation as observed previously for the 0.6 mm sand. The figure also shows that measurements for the coarser particles are slightly lower than those of the 0.6 mm sand. The difference is generally small and could
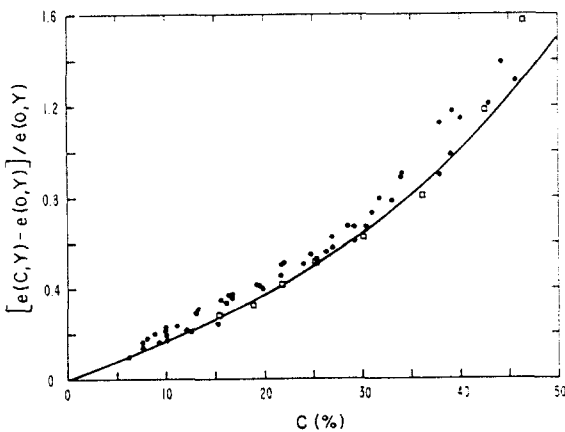

Figure 10. Effect of particle size—sand particles, $d = 1.5$ mm ($\square$), $d = 0.6$ mm ($\bullet$). —, Maxwell's relation; $Y = 0.5$.
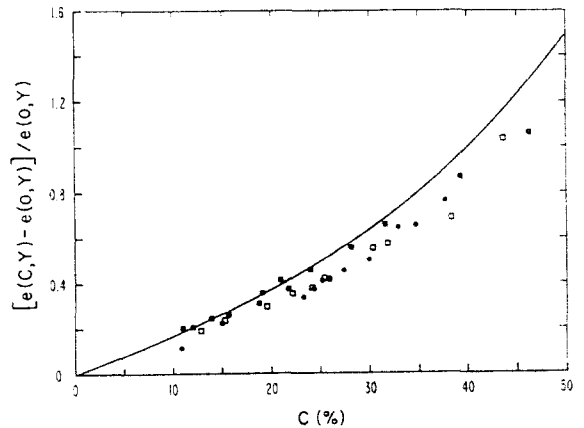

Figure 11. Effect of particle size—glass beads, $d = 5.5$ mm ($\bullet$), $d = 2.8$ mm ($\square$), $d = 1.5$ mm ($\blacksquare$).—, Maxwell's relation; $Y = 0.5$.

probably be neglected, especially if the probe were used to measure the concentration of particles of a wide size distribution.

Figure 11 shows the results obtained for the glass beads. For particles of 1.5 mm mean dia, good agreement with Maxwell's equation was found up to 30% solids concentration. For higher concentrations, the experimental data are significantly lower than Maxwell's equation. For particles of 2.8 mm dia, the experimental results are slightly lower than Maxwell's predictions up to 15% and then start to deviate significantly. For 5.5 mm dia particles, the experimental results are significantly lower than Maxwell's for all concentrations. It is concluded from the results of figures 10 and 11 that particle size has no significant effect for particles of diameter comparable to the sensor electrode spacing and smaller. For coarser particles, particle size has an effect on the calibration curve. As particle size increases, the sensor voltage decreases and it becomes lower than Maxwell's predictions. These results indicate that there is a limitation on the use of a probe with a fixed geometry for measuring solids concentration. This would have to be borne in mind in selecting sensor electrode spacings. The effect is probably due to packing, since as the particle diameter increases the mean concentration at the probe surface will fall.

The next step was to test the probe performance in the pipeline in comparison with accepted methods for measuring solids concentrations: isokinetic sampling and γ-ray absorption methods.

Figure 12 shows the resistivity measured by the conductivity probe and the local concentration measured by the isokinetic sampling method. Measurements were made for slurries of polystyrene particles of 1.4 mm mean dia. Measurements were made by both methods at the pipe center and at radial positions of $R = 0.8$. We see good agreement with calibration results in these tests. One should mention that because the particles used in these experiments were large, no samples could be taken from the center of the pipe at concentrations higher than 35%. Also, no voltage measurements could be taken closer to the pipe wall because particles tended to be trapped between the probe and the wall.

Figure 13 shows a typical sensor voltage profile in the vertical plane. Sand of 0.45 mm mean dia and 10% solids concentration was used in this experiment, at a bulk velocity of 2 m/s and a temperature of 22°C. This shows that the voltage is high at the bottom of the pipe where one expects most of the solids to be found at these operating conditions. The voltage decreases as Y increases and the solids concentration decreases.

Figure 13 also shows the variation of the ballast resistance with position. One observes that this change of resistance is much less than that of the sensor voltage. This difference demonstrates the response of the sensor electrodes to a smaller spatial region than the field electrodes.

The profiles shown in figure 13 are typical for sand–water flows, where because of gravity, more particles are found near the bottom of the pipe. Solids concentrations were obtained from measuring sensor voltages such as those shown in figure 13 and from the calibration curve. This calibration curve was obtained by using a least-squares fit of the experimental data of figure 8.
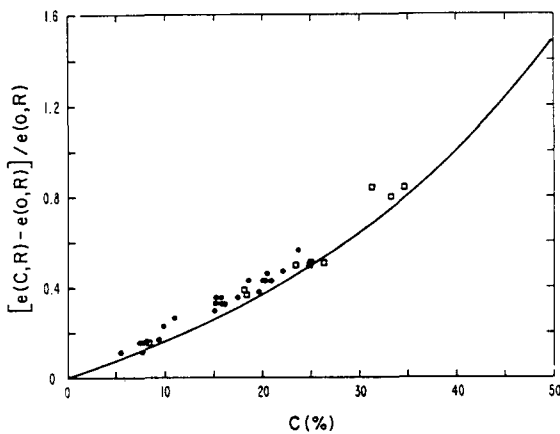

Figure 12. Pipe flow calibration curve using isokinetic sampling and polystyrene particles, $d = 1.4$ mm. —, Maxwell's relation; $\square$, $R = 0.0$; ●, $R = 0.8$.
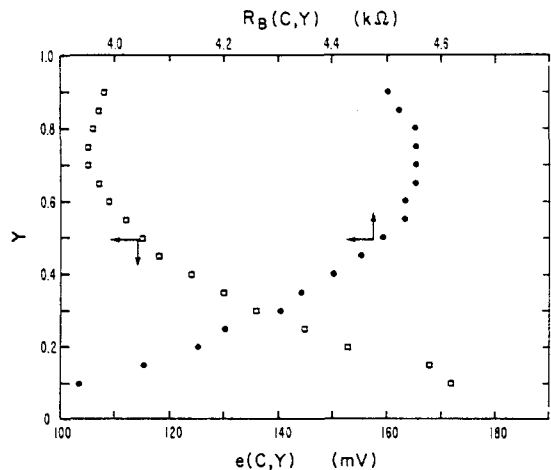

Figure 13. Sensor potential and ballast resistance variations using sand particles, $d = 0.45$ mm; $C_v = 10\%$, $U_b = 2.0$ m/s, $T = 21°C$.
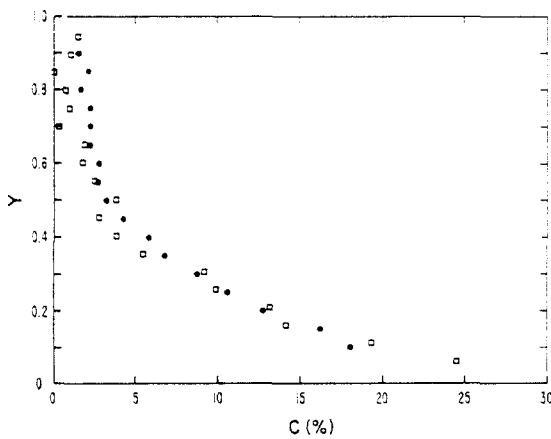
Figure 14. Comparison of concentration profiles obtained with the probe (●) and γ-ray absorption (□) methods using sand particles, $d = 0.19$ mm, at low velocity, $U_b = 2.0$ m/s.
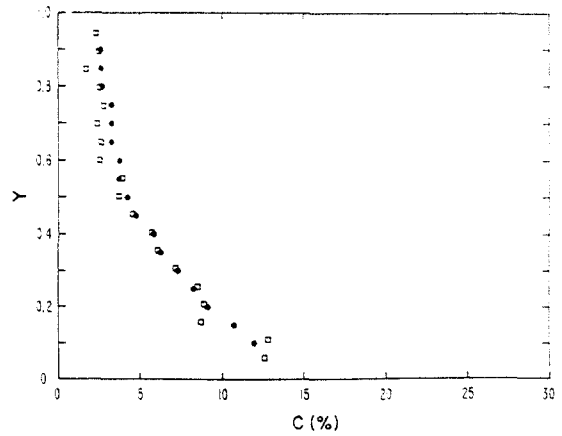

Figure 15. Comparison of concentration profiles obtained with the probe (●) and γ-ray absorption (□) methods using sand particles, $d = 0.19$ mm, at high velocity, $U_b = 3.5$ m/s.

A second test for the probe was conducted using the γ-ray method. Using sand slurries, two scans were done simultaneously, with the conductivity probe and with the γ-ray method. The γ-ray values were obtained with a collimated beam of 1 mm dia.

Figure 14 shows the concentration profile for sand particles of 0.19 mm mean dia and a bulk velocity of 2 m/s. Good agreement between the γ-ray method and probe measurements was obtained. The figure shows some scatter at the top of the pipe where the solids concentration is very low and both methods are subject to error. These results are indirect evidence of a constant concentration across the pipe under the conditions of these measurements.

Figure 15 shows another comparison for the same sand but at a bulk velocity of 3.4 m/s. Again, good agreement was obtained. This result is important because it confirms the results shown in table 3 to the effect that the calibration curve is independent of velocity.

CONCLUSIONS

A simple, economical and accurate method has been developed to measure local *in situ* solids concentration in slurry systems. The experimental results of the present study have shown that:

1. Sensor voltage is symmetrical for a uniform medium as long as one approaches the wall with the same electrode.
2. For non-conducting walls, the effect of position is significant and should be considered. For conducting walls, the wall effect is insignificant if one approaches the wall with the large-area electrode, and consequently no correction is required.
3. Effects of temperature, chemical composition and position were eliminated by using the function $[e(C, Y) - e(0, Y)]/e(0, Y)$.
4. Probe calibration can be done efficiently in a liquid–solid fluidized bed for particles of density greater than that of the liquid.
5. For the probe studied in this work, the calibration curve is independent of velocity.
6. For spherical particles no larger than the spacing of the sensor electrodes, Maxwell's relation can be used to predict solids concentrations.
7. For irregular particles no larger than the electrodes spacing, Maxwell's or Bruggeman's relations can be used at low concentrations. At high concentrations, Bruggeman's relation gives good agreement with the experimental data of the present work.
8. For larger particles, neither Maxwell's nor Bruggeman's relation can predict the experimental results. For these particles, one must either find a calibration curve in a fluidized bed- or use a probe with larger sensor electrode spacing.
9. The probe gives results in agreement with the isokinetic sampling and γ-ray absorption methods.

REFERENCES

BAKER, R. C. & HEMP, J. 1981 Slurry concentration meters state of the art: review and bibliography. *BHRA Fluid Engng Ser.* **8**, 3–25.

BECK, M. S., CALVERT, G., HOBSON, J. H., LEE, K. T. & MENDIES, P. J. 1971 Total volume and component flow measurement in industrial slurries and suspensions using correlation techniques. *Measur. Control* **4**, 133–138.

BECK, M. S., MENDIES, P. J., WALECKI, T. & GATLAND, H. B. 1974 Measurement and control in hydraulic transport systems using cross-correlation measurement systems and fluidic diverters. *Hydrotransport 3, Proc 3rd Int. Conf. on the Hydraulic Transport of Solids in Pipes*, Paper F3, pp. 69–80. BHRA Fluid Engineering, Cranford, Beds., U.K.

BECK, M. S., GREEN, R. G, HAMMER, E. A. & THORN, R. 1983 On-line multi-component flow measurement. *Symp. on Flow Metering and Proving Technology in the Offshore Oil Industry.* pp. 1–12. Inst. of Measurement and Control.

BEGOVICH, J. M. & WATSON, J. S. 1978 An electroconductivity technique for the measurement of axial variation of holdups in three-phase fluidized beds. *AICHE J.* **24**, 351–354.

BRUGGEMAN, D. A. G. 1935 Berechnung Verschiedener Physicalischer Konstanten von Heterogenen Substanzen. *Annln Phys.* **24**, 636.

CYBULA, C. J. 1971 An investigation of the measurement of void-fraction in air–water mixtures by the electrical impedance method AAEC Research Establishment, Lucas Heights, Australia, Report No. 592, pp. 1–20.

DEBRECZENI, E., MEGGYES, T. & TARJAN, I. 1978 Measurement methods in an experimental rig for hydraulic transport. *Hydrotransport 5, Proc. 5th Int. Conf. on the Hydraulic Transport of Solids in Pipes*, Paper G1, pp. 1–19. BHRA Fluid Engineering, Cranford, Beds., U.K.

DE LA RUE, R. E. & TOBIAS, C. W. 1959 On the conductivity of dispersions. *J. electrochem. Soc.* **106**, 827.

GREEN, R. G. & CUNLIFFE, J. M. 1983 A frequency-modulated capacitance transducer for on-line measurement of two-component fluid flow. *Measurement* **1**, 191–195.

HASHIN, Z. 1968 Assessment of the self consistent scheme approximation: conductivity of particulate composites. *J. composite Mater.* **2**, 284–300.

KAKKA, R. S. & PHIL, M. 1974 Review of instruments for measuring flow rate and solids concentrations in steel works slurry pipelines. *Hydrotransport 3, Proc. 3rd Int. Conf. on the Hydraulic Transport of Solids in Pipes*, Paper F6, pp. 81–92. BHRA Fluid Engineering, Cranford, Beds., U.K.

KAO, D. T. & KAZANSKIJ, I. 1979 On slurry flow velocity and solid concentration measuring techniques. *Proc. 4th. Int. Tech. Conf. on Slurry Transportation, pp.* 102–120. Slurry Transportation Association, Las Vegas, Nev.

KESKA, J. 1978 Measurement of the distribution and overall spatial solid body content of mixtures in pipelines. *Hydrotransport 5, Proc. 5th Int. Conf. on the Hydraulic Transport of Solids in Pipes*, Paper G5, pp. 59–72. BHRA Fluid Engineering, Cranford, Beds., U.K.

LEE, K. T., BECK, M. S. & McKEOWN 1974 An on-line instrument for measuring small quantities of dispersed non-conducting liquid in a conducting liquid. *Measur. Control* **7**, 341–345.

MACHON, V., FORT, I. & SKRIVANEK, J. 1982 Local solids distribution in the space of a stirred vessel. *Proc. 4th Eur. Conf. on Mixing*, Paper B3, pp. 289–302. BHRA Fluid Engineering, Cranford, Beds., U.K.

MAXWELL, J. C. 1881 *A Treatise on Electricity and Magnetism.* Calender Press, Oxford.

MERILO, M., DECHENE, R. L. & CICHOWLAS, W. M. 1977 Void fraction measurement with a rotating electric field conductance gauge. *J. Heat Transfer* **99**, 330–332.

NASR-EL-DIN, H. & SHOOK, C. A. 1985 Sampling from slurry pipelines: thick-walled and straight probes. *J. Pipelines* **5**, 113–124.

NASR-EL-DIN, H., SHOOK, C. A. & ESMAIL, M. N. 1984 Isokinetic probe sampling from slurry pipelines. *Can. J. chem. Engng* **62**, 179–185.

NEALE, G. H. & NADER, W. K. 1973 Prediction of transport processes within porous media:

diffusive flow processes within an homogeneous swarm of spherical particles. *AIChE Jl* **19**, 112–119.

ONG, K. H. & BECK, M. S. 1975 Slurry flow velocity, concentration and particle size measurement using flow noise and correlation techniques. *Measur. Control* **8**, 453–463.

PERRY, R. H. & CHILTON, C. H. 1973 *Chemical Engineer's Handbook*, 5th edn, pp. 3–243. McGraw-Hill, New York.

SCARLETT, B. & GRIMLEY, A. 1974 Particle velocity and concentration profiles during transport in a circular pipe. *Hydrotransport 3, Proc. 3rd Int. Conf. on the Hydraulic Transport of Solids in Pipes*, Paper D3, pp. 24–37. BHRA Fluid Engineering, Cranford, Beds., U.K.

STANLEY-WOOD, N. G., LIEWELLYN, G. J. & TAYLOR, A. 1981 On-stream particle size, concentration and velocity measurements by auto-correlation of scattered laser light. *Powder Technol.* **29**, 217–223.

SUBBOTIN, V. I., POKHVALOV, Y. E., MIKHAILOV, L. E., LEONOV, V. A. & KRONIN, I. V. 1974 Resistance and capacitance methods of measuring steam content. *Teploenergetika* **21**, 63–68.

TURNER, J. C. R. 1973 Electrical conductivity of liquid-fluidized beds. *AIChE Symp. Ser.* **69**(128), 115–122.

TURNER, J. C. R. 1976 The electrical conductance of liquid-fluidized beds of spheres. *Chem. Engng Sci.* **31**, 487–492.